

**\*\*Volume Title\*\***  
**ASP Conference Series, Vol. \*\*Volume Number\*\***  
**\*\*Author\*\***  
 © **\*\*Copyright Year\*\*** *Astronomical Society of the Pacific*

## Strange mode instability for micro-variations in Luminous Blue Variables

Hideyuki Saio<sup>1</sup>, Cyril Georgy<sup>2</sup>, and Georges Meynet<sup>3</sup>

<sup>1</sup>*Astronomical Institute, Graduate School of Science, Tohoku University, Sendai, Japan*

<sup>2</sup>*Centre de Recherche Astrophysique de Lyon, École Normale Supérieure de Lyon, 46, allée d'Italie, 69384 Lyon Cedex 07, France;*  
*Astrophysics, Lennard-Jones Laboratories, EPSAM, Keele University, ST5 5BG, Staffordshire, UK*

<sup>3</sup>*Geneva Observatory, University of Geneva, Maillettes 51, 1290 Sauverny, Switzerland*

**Abstract.** If a massive star has lost significant mass during its red-supergiant stage, it would return to blue region in the HR diagram and spend a part of the core-He burning stage as a blue supergiant having a luminosity to mass ratio ( $L/M$ ) considerably larger than about  $10^4$  (in solar units); the duration depends on the degree of internal mixing and on the metallicity. Then, various stellar pulsations are excited by enhanced  $\kappa$ -mechanism and strange mode instability. Assuming these pulsations to be responsible for (at least some of) the quasi-periodic light and radial-velocity variations in  $\alpha$  Cygni variables including luminous blue variables (LBVs; or S Dor variables), we can predict masses and surface compositions for these variables, and compare them with observed ones to constrain the evolutionary models. We discuss radial pulsations excited in evolutionary models of an initial mass of  $40 M_{\odot}$  with solar metallicity of  $Z = 0.014$ , and compare them to micro-variations in the two Galactic LBVs, HR Car and HD 160529. We have found that these stars should have lost more than half of the initial mass and their surface CNO abundances should be significantly modified from the original ones showing partial H-burning products.

### 1. Introduction

Many luminous blue supergiants, including Luminous Blue Variable (LBV, or S Dor variable) stars, show semi-periodic micro-variations in brightness and radial velocities, sometimes superposed on long-timescale variations (S Dor phases; e.g., Lamers et al. 1998). The micro-variations are attributed to stellar pulsations, and these variables are called  $\alpha$  Cygni variables. They are known to be present in our Galaxy, Magellanic clouds (e.g., van Leeuwen et al. 1998), and even in the nearby galaxy NGC 300 (Bresolin et al. 2004). Fig. 1 shows approximate positions of some of the  $\alpha$  Cygni variables on the HR diagram. They are broadly distributed in the B-A supergiant region of  $L \gtrsim 10^5 L_{\odot}$ , in stark contrast to the distributions of classical variables confined to narrow strips bounded by  $T_{\text{eff}}$ s. The latter property comes from the weakly nonadiabatic pulsations excited by  $\kappa$ -mechanisms around opacity peaks (e.g., Cox 1980), while

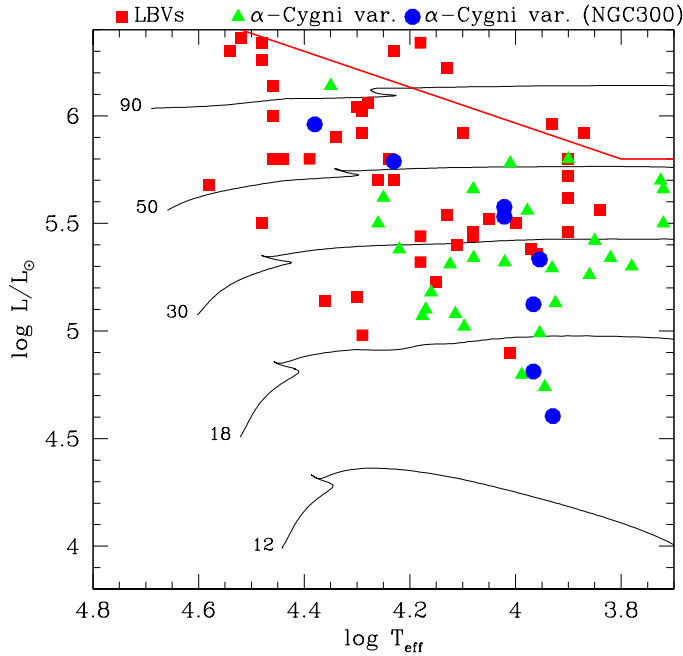


Figure 1. Approximate positions of  $\alpha$  Cygni variables and LBV (S Dor) stars on the HR diagram. Straight lines in the upper-right part indicate the HD limit (Humphreys & Davidson 1979). Observational parameters are adopted from van Genderen (2001) for LBV stars, van Leeuwen et al. (1998) for other  $\alpha$  Cygni variables in our Galaxy, LMC and SMC. The parameters of the variables in NGC 300 are adopted from Bresolin et al. (2004) and Kudritzki et al. (2008).

the distribution of the  $\alpha$  Cygni variables indicate the semi-periodic micro variations to be extremely nonadiabatic pulsations of stars with very high luminosity to mass ratios ( $L/M \gtrsim 10^4 L_\odot/M_\odot$ ) involving strange modes (e.g., Saio 2009; Saio et al. 2013). For the evolution models of massive stars evolving toward the red-supergiant for the first time, however, such a high  $L/M$  ratio occurs only for initial masses larger than  $\sim 60 M_\odot$  and hence the excitation of radial pulsations is expected only for luminosities of  $\log L/L_\odot \gtrsim 5.8$  (Kiriakidis et al. 1993; Saio 2011); i.e., these models fail to explain the distribution of the  $\alpha$  Cygni variables, which extends down to  $\log L/L_\odot \approx 4.6$  (Fig. 1).

Recent evolution models including rotational mixing and updated wind mass-loss rates (Ekström et al. 2012), however, indicate that stars with masses larger than  $\sim 20 M_\odot$  return to blue supergiant region (blue loop) after considerable mass is lost during the red-supergiant stage (the mass limit can be as low as  $\sim 12 M_\odot$  if the mass-loss rates in the red-supergiant stage is enhanced greatly; Georgy 2012). Significant mass loss makes the  $L/M$  ratio on the blue loop much higher than that during the first crossing, so that radial/nonradial pulsations can be excited if  $\log L/L_\odot \gtrsim 4.7$  (Saio et al. 2013), which is roughly consistent with the distribution of the  $\alpha$  Cygni variables on the HR diagram. Comparing with relatively less luminous  $\alpha$  Cygni variables, Saio et al.

(2013) found that the excited periods are roughly consistent with most of the observed period ranges, although the predicted surface N/C and N/O ratios seem too high at least for Rigel and Deneb.

In this paper, we discuss radial pulsations of slightly more luminous  $\alpha$  Cygni variables with S Dor type long-timescale variations (i.e., LBVs).

## 2. Evolution of massive stars and the excitation of radial pulsations in LBVs

One useful property of the  $\alpha$  Cygni type variations in LBVs is that the period changes depending on the long-timescale S Dor phase; generally, the period is longer in visually brighter (i.e., cooler) phases as discussed in Lamers et al. (1998); the bolometric luminosity is thought to be approximately constant during the S Dor phase. This phenomenon is consistent with interpreting the micro-variations by stellar pulsation, of which period gets longer when the radius increases.

Among the three Galactic LBVs discussed in Lamers et al. (1998) we select two LBVs, HR Car and HD 160529, which have luminosities of  $\log L/L_{\odot} \approx 5.5$  comparable with luminosities during the blue-loop evolution of our  $M_i = 40 M_{\odot}$  ( $M_i$  = initial mass) model as shown in the top panel of Fig. 2. The ranges of  $\log T_{\text{eff}}$  connected with horizontal lines indicate the ranges of temperature variations during long-timescale S Dor phases.

As we can see in Fig. 2, during the evolution toward the red-supergiant region after the main-sequence evolution (1st crossing), no radial pulsations are excited in the blue-supergiant region ( $4.35 \gtrsim \log T_{\text{eff}} \gtrsim 3.85$ ). The model returns to blue during core He burning after losing considerable mass in the red-supergiant stage (Fig. 2 bottom panel), and then radial pulsations are excited. During the final blueward evolution, the model has a luminosity of  $\log L/L_{\odot} \approx 5.55$  comparable with the two LBVs. In this phase of evolution, three radial pulsation modes are excited, and their periods and the dependences on the effective temperature are roughly consistent with the observed periods and their variations during the S Dor phases of HR Car and HD 160529 (middle panel of Fig. 2). This indicates that these two LBVs would have already lost significant mass from the initial one ( $40 \rightarrow 17 M_{\odot}$  in our model).

Because of the large mass loss, the surface composition is modified, as layers where partial H-burning through CNO cycle occurred are progressively uncovered (bottom panel of Fig. 2). Since this model does not include rotational mixing, and since this model does not reach very low  $T_{\text{eff}}$  where very deep convective zone can develop, the major driver of the evolution of the surface chemical composition is the mass loss. As shown in Fig. 2, there are three major mass loss episodes, two at a  $T_{\text{eff}} \sim 3.6$ , and one at a  $T_{\text{eff}} \sim 4.1$  (corresponding to the temperature of the bi-stability jump in the stellar wind where a sharp transition occurs in the mass-loss rates (Vink et al. 2000)). Most of the modification of the surface chemical composition occurs during the first strong mass-loss episode, where the star loses  $\sim 10 M_{\odot}$ , before the blue loop starts. The second mass-loss episode ( $\sim 5 M_{\odot}$  lost) changes again slightly the surface composition at the tip of the loop. The last mass-loss episode, in the red part of the HRD, allows the star to evolve definitively towards the blue side of the HRD, but does not change the surface composition any more.

Our model predicts  $X_{\text{H}} = 0.41$ ,  $X_{\text{N}}/X_{\text{C}} = 1.1 \times 10^2$ , and  $X_{\text{N}}/X_{\text{O}} = 9.7$  for the two LBVs, where  $X_i$  means the mass fraction of element  $i$  on the stellar surface. The surface hydrogen abundance corresponds to a number ratio of  $\text{He}/\text{H} \approx 0.35$ , which is

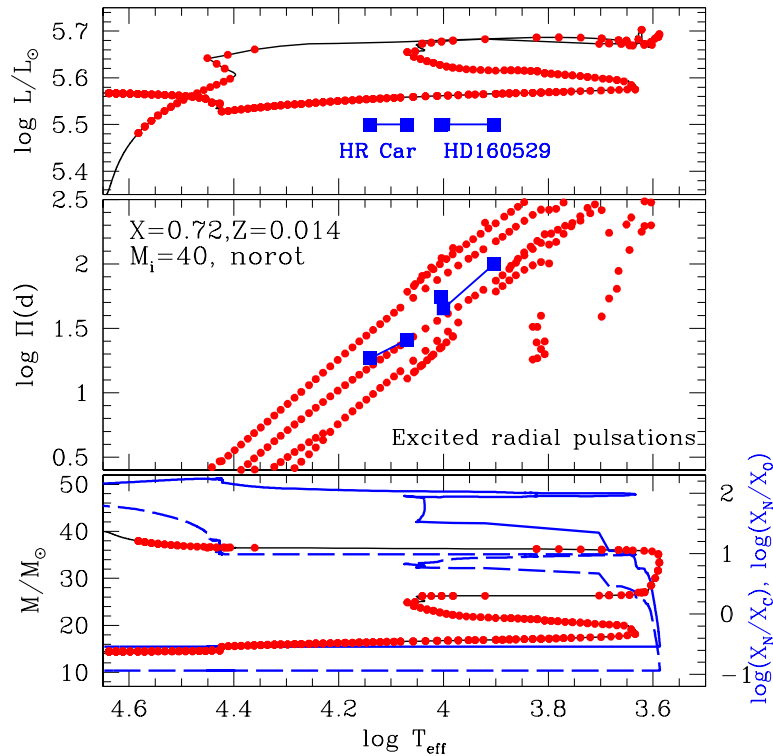


Figure 2. **Top panel:** Evolutionary track on the HR diagram of a non-rotating model with an initial mass of  $40M_{\odot}$ , in which a core overshooting of 0.1 pressure scale height is included, and the wind mass loss is included in the same way described in Ekström et al. (2012). Approximate positions of two galactic LBVs, HR Car and HD 160529, are plotted, where parameters are adopted from Lamers et al. (1998) and Stahl et al. (2003). The effective temperature ranges connected with horizontal lines indicate approximate ranges of variations during long-timescale S Dor phases. Small red dots along the evolutionary track indicate models in which at least one radial pulsation is excited. **Middle panel:** Periods ( $\Pi$ ) of excited radial pulsations as function of  $T_{\text{eff}}$  are compared with period ranges of the micro-variations of the two LBVs shown in the top panel. Periods are adopted from Lamers et al. (1998) and Stahl et al. (2003). **Bottom panel:** The variations of total mass (black line) and of surface abundance ratios,  $\log(X_N/X_C)$  (blue solid line) and  $\log(X_N/X_O)$  (blue dashed line). The surface abundance ratios generally increase with evolution so that the post RSG phase corresponds to the upper part of the curves (see the blue scale on the right). The red dots have the same meaning as in the top panel. They indicate pulsations are excited in blue supergiants only after the mass is decreased considerably.

comparable to the photospheric value of P Cyg (another Galactic LBV), 0.40, listed in Lamers et al. (2001); P Cyg has a luminosity  $\log L/L_{\odot} = 5.8$  comparable to our model. Our surface  $X_N/X_O$  ratio corresponds to a number ratio of about 11, which is higher than the ratios ( $\leq 6 \pm 2$ ) in the nebulae around LBV stars discussed in Lamers et al.

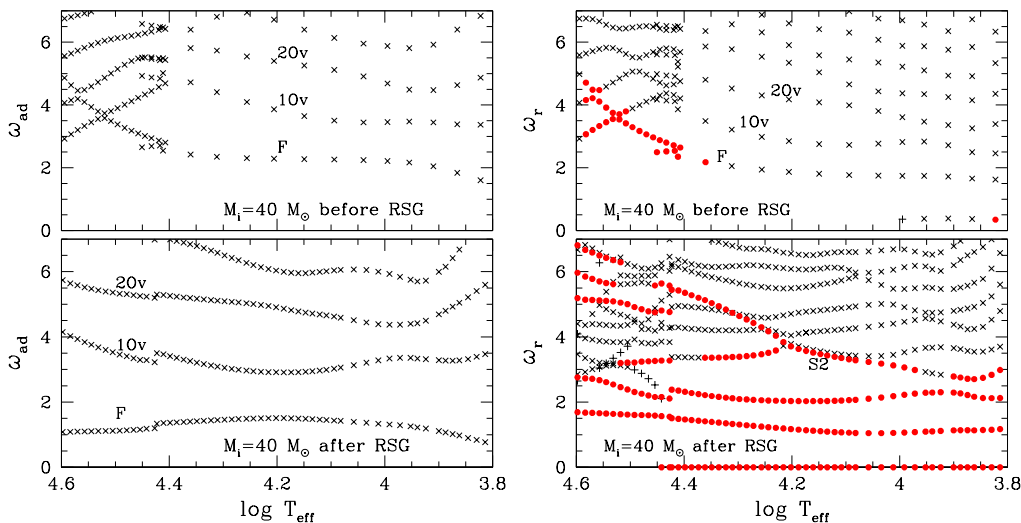


Figure 3. Pulsation frequencies normalized by  $\sqrt{GM/R^3}$  are plotted as a function of effective temperature for models in the main-sequence stage and evolving to red-supergiant stage for the first time (top panels) and for models evolving blueward for the 2nd time (4th crossing; bottom panels). The left panels show adiabatic frequencies and the right panels show non-adiabatic ones (the real part of eigenfrequencies;  $\omega_r$ ). Red dots indicate excited modes and crosses indicate damped modes. In the left panels for adiabatic pulsations and in the top-right panel, fundamental (F), first overtone (10v) and second overtone (20v) modes are indicated, but not in the bottom-right panel, because in the 4th crossing models, pulsations are so non-adiabatic that mode identifications are not possible. The symbol ‘S2’ indicates genuine strange modes which exist even in the limit of diminishing thermal time. Note that along the sequence of excited modes, damped modes tend to have similar frequencies, which form approximately complex-conjugate pairs (see the top-left panel of Fig. 4).

(2001). The difference might not be serious, because the ratio in nebulae should be considered as a lower bound for the photospheric value, and the observed values might still be affected by considerable uncertainties. In addition, our present model does not include rotational mixing, which might change considerably the surface CNO ratios in the LBV stage.

### 3. Property of very nonadiabatic pulsations of LBVs

Fig. 3 shows pulsation frequencies of several modes normalized by  $\sqrt{GM/R^3}$  as a function of effective temperature along the evolutionary track of  $M_i = 40 M_\odot$  model during main-sequence and the post-main sequence (1st crossing) evolution in the top panels, and during the final blueward evolution in the bottom panels. The left and right panels show adiabatic and nonadiabatic frequencies, respectively. Adiabatic pulsation modes are well ordered from lowest to higher frequencies as fundamental (F), 1st overtone (10v), 2nd overtone (20v), etc even in the advanced evolution stage. However, the ordering is destroyed by strong nonadiabatic effects as in the model on the final blue-

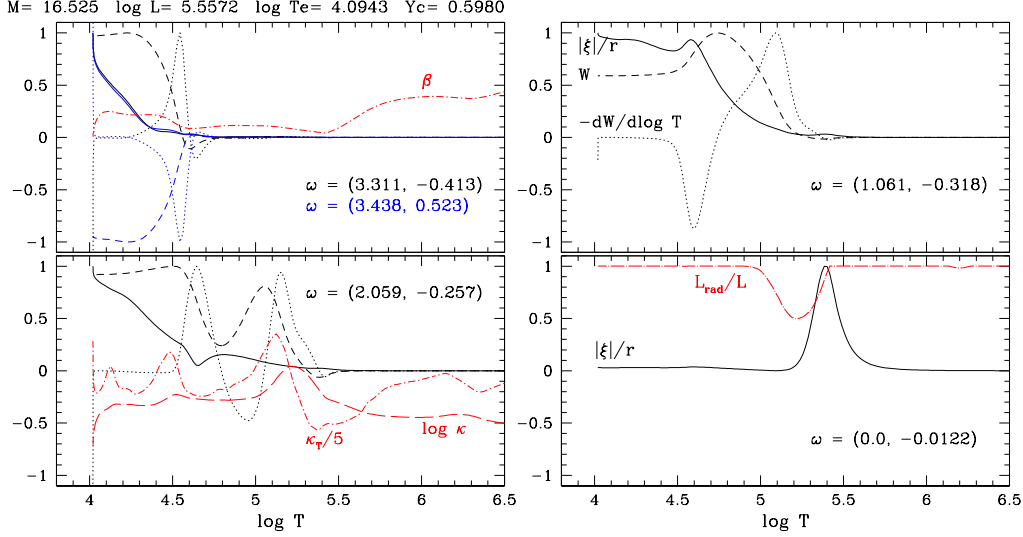


Figure 4. Profiles of displacements  $|\xi|/r$  (solid lines), and work,  $W(r)$  (dashed lines), and differential work,  $-dW/d \log T$  (dotted lines), are shown for the four lowest frequency modes in the model evolving blueward (right-bottom panel of Fig. 3) at  $\log T_{\text{eff}} = 4.09$ . Layers with  $-dW/d \log T > 0$  drive the pulsation, and the pulsation is excited if the work  $W$  is positive at the surface (see Saio et al. 2013, for the definition of  $W$ ). The blue lines in the top-left panel are for a (damped) mode nearly complex-conjugate of the excited one shown by black lines. Note that the blue line for the displacement  $|\xi|/r$  is nearly superposed on the black line, and the works and the differential works for the two modes are nearly mirror-symmetric. Red lines show profiles of  $\beta = P_{\text{gas}}/P$ , opacity  $\kappa$  and its derivative with respect to the temperature,  $\kappa_T \equiv d \ln \kappa / d \ln T$ , and the ratio of the radiative to total luminosity  $L_{\text{rad}}/L$ .

ward evolution (right-bottom panel of Fig. 3), in which it is not possible to assign the correspondence between adiabatic and nonadiabatic modes.

Nonadiabatic (real parts of ) frequencies of excited modes are plotted by red dots (damped modes by crosses). The right-bottom panel of Fig. 3 indicates that during the blue-supergiant phase on the blue loop three pulsation modes and one monotonic mode ( $\omega_r = 0$ ) are excited. Note that the sequence denoted as S2 consists, in most part, two modes having similar pulsations frequencies ( $\omega_r$ ) but one is excited and the other damped. These two modes approximately form a complex-conjugate pair; this is the property of genuine strange-mode instability in the extremely nonadiabatic condition with diminishing thermal time (NAR condition; Gautschy & Glatzel 1990).

Fig. 4 shows some of the properties of the excited modes and the damped complex-conjugate mode in the model at  $\log T_{\text{eff}} = 4.094$  on the final blueward track (the mass is reduced to  $16.5 M_{\odot}$ ). The top-left panel is for the S2 pair modes; black lines for excited modes and blue lines for damped modes. The listed complex frequencies indicate that these modes are indeed nearly complex-conjugate to each other. Amplitude profiles of these modes are nearly identical and confined to the second He ionization zone and above where the radiation pressure is dominant ( $\beta = P_{\text{gas}}/P \ll 1$ ) and the thermal time

is very small; this explains why these modes have extreme nonadiabatic strange-mode property.

The mode shown in the left-bottom panel is excited by enhanced  $\kappa$ -mechanism at He II ionization zone ( $\log T \approx 4.6$ ) and at the Fe opacity bump ( $\log T \approx 5.2$ ), and the mode in the right-top panel is excited at the Fe opacity bump.

The amplitude of the mode shown in the right-bottom panel of Fig. 4 monotonically grows; i.e. a small deviation from the equilibrium state grows monotonically, although the growth time is some thirty times longer than that of the excited pulsation modes. (Such monotonically growing modes were also found in first crossing models of  $M_i \geq 60 M_\odot$ ; Saio 2011) This mode has a large amplitude around  $\log T \sim 5.4$  slightly deeper than layers where the Fe-opacity bump resides. The significance of the monotonic modes in massive star phenomena is not clear.

#### 4. Conclusion

We discussed radial pulsations excited in evolutionary models of  $M_i = 40 M_\odot$  and found that the pulsations are excited during the blueward evolution after the mass has been reduced to  $\sim 17 M_\odot$ . They seem consistent with the periods and their variations of the micro variations observed in the two Galactic LBVs, HR Car and HD 160529. This indicates that these stars should have already lost significant mass, and the surface compositions should have been modified significantly from the original ones showing partially processed H-burning products.

Finally, we note that pulsations might be able to significantly affect mass loss rates in LBV (and pre-LBV) stars. For example, the nonlinear pulsation analysis by Glatzel et al. (1990) for a supergiant model of  $64 M_\odot$  ( $M_i = 120 M_\odot$ ) indicates that the photospheric velocities of pulsation can reach to the escape velocity. Observationally, on the other hand, Aerts et al. (2010) found that the mass loss rates of the luminous ( $\log L/L_\odot \approx 6.1$ ) blue supergiant HD 50064 change on a time scale similar to the period of photospheric variations, indicating connection between pulsation and mass loss. Further theoretical and observational investigations on the interaction between pulsation and mass loss in massive stars would be important.

**Acknowledgments.** CG acknowledges support from EU-FP7-ERC-2012-St Grant 306901.

#### References

- Aerts, C., Lefever, K., Baglin, A., Degroote, P., Oreiro, R., Vučković, M., Smolders, K., Acke, B., Verhoelst, T., Desmet, M., Godart, M., Noels, A., Dupret, M.-A., Auvergne, M., Baudin, F., Catala, C., Michel, E., & Samadi, R. 2010, *A&A*, 513, L11
- Bresolin, F., Pietrzyński, G., Gieren, W., Kudritzki, R.-P., Przybilla, N., & Fouqué, P. 2004, *ApJ*, 600, 182
- Cox, J. 1980, *Theory of stellar pulsation* (Princeton: Princeton University Press)
- Ekström, S., Georgy, C., Eggenberger, P., Meynet, G., Mowlavi, N., Wyttenbach, A., Granada, A., Decressin, T., Hirschi, R., Frischknecht, U., Charbonnel, C., & Maeder, A. 2012, *A&A*, 537, A146
- Gautschi, A., & Glatzel, W. 1990, *MNRAS*, 245, 597
- Georgy, C. 2012, *A&A*, 538, L8
- Glatzel, W., Kiriakidis, M., Chernigovskij, S., & Fricke, K. 1990, *MNRAS*, 245, 597
- Humphreys, R., & Davidson, K. 1979, *ApJ*, 232, 409

- Kiriakidis, M., Fricke, K., & Glatzel, W. 1993, *MNRAS*, 264, 50
- Kudritzki, R.-P., Miguel, A., Bresolin, F., Przybilla, N., Gieren, W., & G., P. 2008, *ApJ*, 681, 269
- Lamers, H., Bastiaanse, M., Aerts, C., & Spoon, H. 1998, *A&A*, 335, 605
- Lamers, H., Nota, A., Panagia, N., Smith, L., & Langer, N. 2001, *ApJ*, 551, 764
- Saio, H. 2009, *CoAst*, 158, 245
- 2011, *MNRAS*, 412, 1814
- Saio, H., Georgy, C., & Meynet, G. 2013, *MNRAS*, in press
- Stahl, O., Gäng, T., Sterken, C., Kaufer, A., Rivinius, T., Szeifert, T., & Wolf, B. 2003, *A&A*, 400, 279
- van Genderen, A. 2001, *A&A*, 366, 508
- van Leeuwen, F., van Genderen, A., & Zegelaar, I. 1998, *A&AS*, 128, 117
- Vink, J., de Koter, A., & Lamers, H. 2000, *A&A*, 362, 295